Identification of BRAF Inhibitors through In Silico Screening

Cheng Luo,[†,§,||] Peng Xie,[†,‡,||] and Ronen Marmorstein*[,†,‡]

The Wistar Institute and Department of Chemistry, University of Pennsylvania, Philadelphia, Pennsylvania 19104

Received May 9, 2008

The BRAF protein kinase, a molecule in the RAS-RAF-MEK-ERK signaling pathway, is mutated to harbor elevated kinase activity in ~7% of human cancers, which makes it an important therapeutic target for inhibition. Several BRAF protein-kinase inhibitors have been developed through high-throughout screening in vitro; however, many of these compounds suffer from a lack of suitable kinase specificity and other chemotherapeutic properties. In silico screening has evolved as a powerful complimentary approach to protein-kinase inhibitor identification. Here we describe an in silico screen for BRAF inhibitors that leads to the identification of a series of purine-2,6-dione analogues with IC_{50} values in the single-digit micromolar range and with significant selectivity for BRAF over other representative protein kinases. The binding modes of these inhibitors to BRAF are analyzed through molecular docking to derive structure−activity relationships and to assist in the future development of more potent and more specific BRAF inhibitors.

Introduction

The RAS-RAF-MEK-ERK[a] (MAPK) signaling pathway plays a central role in transducing signals from extracellular growth factors to the nucleus to promote cell proliferation and survival. The MAPK pathway also represents a common pathway that is activated at aberrantly high levels in a variety of human cancers. RAF protein kinases are central players in the MAPK signal transduction pathway and have been shown to be critical for mediating cell proliferation, survival, and angiogenesis in various cancer models.[1] The RAF protein kinase family consists of three isoforms named ARAF, c-RAF-1, and BRAF. Earlier functional studies on the RAF family focused on c-RAF-1, and these studies revealed that RAF kinases are tightly regulated and require multiple phosphorylation events from diverse upstream protein kinases to achieve kinase activation. The importance of BRAF activation was highlighted by a more recent study that showed that it is mutated in approximately 7% of human cancer,[2] most notably in melanoma (50−70%), ovarian (~35%), thyroid (~30%), and colorectal (~10%) cancers. Among the many activating BRAF mutations that were identified in human cancers, a single V600E mutation within the BRAF kinase domain accounts for over 90% of all of these mutations, and the $BRAF^{V600E}$ mutant protein was found to be 500 times more active than the wild-type protein in vivo.[3] Oncogenic $BRAF^{V600E}$ bypasses the requirement for upstream regulation by phosphorylation that results in a MAPK signaling pathway that is constitutively activated in the absence of extracellular growth factor signals. These data strongly implicate the BRAF protein kinase as an important target for the development of small molecule inhibitors in the treatment of human cancers, particularly melanoma.

Toward the preparation of BRAF inhibitors, the general RAF protein-kinase inhibitor sorafenib (BAY439006) was developed through high-throughput solution screening (HTS), and it was approved by the FDA for use in renal carcinoma,[4] although this compound failed to show therapeutic activity in the treatment of malignant melanoma. Whereas several other BRAF inhibitors that were identified through HTS are currently in various stages of development, the discovery of novel, potent, and specific inhibitors against BRAF protein kinase remains a major challenge.

Because of the cost-inefficient and time-consuming process of conventional drug discovery over the past decade, high-throughput virtual screening (HTVS) has emerged as an attractive and complementary approach to traditional HTS. HTVS typically depends on the availability of a high-resolution crystal structure of the protein target as a template for computational screening. Over the years, HTVS has been applied to the successful identifications of biologically active molecules against targets such as HIV-1 protease, thymidylate synthase, influenza hemagglutinin, and parasitic proteases.[5,6] The availability of the crystal structure of the BRAF protein kinase[3,7] now provides an opportunity for utilizing the HTVS strategy to identify BRAF inhibitors. Here we describe an HTVS approach to identify a series of novel inhibitors against the BRAF protein kinase. Specifically, we screened about 90 000 low-molecular-weight compounds from a publicly available small molecule database using the HTVS approach, and after two generations of optimization from a primary inhibitor lead, we developed a novel series of compounds with IC_{50} values in the single-digit micromolar range against BRAF kinase. We also show that these compounds display selectivity for the inhibition of BRAF over other representative protein kinases, and we employ molecular docking of these compounds bound to BRAF to derive structure−activity relationships (SARs). These results establish that virtual screening is an effective strategy for the discovery of potent and selective BRAF inhibitors, and we

* To whom correspondence should be addressed. Tel: 215-898-5006. Fax: 215-898-0381. E-mail: marmor@wistar.org.

† The Wistar Institute.

‡ Department of Chemistry, University of Pennsylvania.

§ Current Address: Drug Discovery and Design Center, Shanghai Institute of Materia Medica, Shanghai 201203.

|| C.L. and P.X. equally contributed to this study.

[a] Abbreviations: RAS, small G protein Ras; RAF, RAF proto-oncogene serine/threonine protein kinase; MEK, dual-specificity mitogen-activated protein kinase; ERK, extracellular signal-regulated kinase; MAPK, mitogen-activated protein kinase; PI3Kγ, phosphatidyl-inositol-3-kinase gamma isoform; GSK3β, glycogen synthase kinase 3 beta isoform; Pim1, proto-oncogene serine/threonine protein kinase Pim1; MST1, STE20-like kinase MST1; PAK, p21-activated kinase; CMGC, CDK/MAPK/GSK3/CDK-like protein kinase family; CAMK, calcium/calmodulin-dependent kinase family; STE, ste20-like protein kinase family.

10.1021/jm800539g CCC: $40.75
Published on Web 09/11/2008

provide a novel lead scaffold for the future design of more potent and more specific $BRAF^{WT}$ and $BRAF^{V600E}$ protein-kinase inhibitors.

Results and Discussion

High-Throughout Virtual Screening Procedure. In this procedure, residues within a distance of 6 Å around the BRAF inhibitor **50** (SB590885)[7] were isolated for the construction of a grid for screening by the use of the DOCK4.0 program.[8] This grid was large enough to include every residue of the BRAF kinase ATP-binding pocket. To create a library of compounds for screening, we selected a public database that contained a large number of small molecule compounds that would be available for subsequent solution screening at a nominal cost. To this end, we selected the SPECS database that contained about 300 000 small-molecule compounds. To refine the database further to include the compounds that were likely to be soluble in an aqueous solution to allow for a follow-up solution assay, we filtered the database for compounds with a log *S* value of greater than 4, which resulted in a database of about 90 000 small-molecule compounds. To screen these compounds efficiently within a reasonable time, we initially used DOCK4.0,[8] a docking program that had already been successfully used for the identification of inhibitors for the HIV-1 protease, thymidylate synthase, influenza hemagglutinin, and parasitic proteases, as the primary molecular docking program,[5] As a pilot study to test the effectiveness of our docking procedure, we included two known BRAF inhibitors **50** and **51** (sorafenib)[3] as positive controls for this docking procedure in an initial trial run with 998 randomly selected compounds from the SPECS database. As expected, these two inhibitors were placed as the top two scoring compounds in this docking procedure. We then carried out docking against the remaining compounds, and the top 5000 hits that were generated from the energy scoring function of DOCK4.0 were docked using three other docking programs that employed different scoring functions. XScore (version 1.2.1) was used for calculating a binding score for a given protein−ligand complex structure,[9] SLIDE (version 2.3.1) was used for the calculation of hydrogen bonds and the hydrophobic complementarity while considering the flexibility of both protein and ligand,[10,11] and AutoDock3.0 was used for calculating the free energy of binding.[12] Specifically, the XScore program was first carried out on the top 5000 candidate compounds that were generated from DOCK4.0. The top 2000 compounds from XScore were then selected for reevaluation by the use of the SLIDE scoring function. The top 783 compounds from SLIDE were finally evaluated according to the free energy of binding with the AutoDock3.0 program. According to their binding modes, free-energy scores, and scaffold diversity, 20 compounds from 10 manually classified groups were selected (Table S1 in the Supporting Information) for BRAF inhibition solution studies by the use of an ELISA-based activity assay system.

In Vitro Analysis of BRAF Inhibitors Identified through Virtual Screening. Eighteen virtual screening hits (compounds **1**−**18**) that are shown in Table S1 and Figure S1a of the Supporting Information were assayed for BRAF activity at an inhibitor concentration of 100 μM by the use of an ELISA-based MEK phosphorylation assay. From this initial screen, only compound **1** reduced BRAF kinase activity (to about 80% of wild-type activity), and a subsequent measurement of the dose−response inhibition curve of compound **1** against BRAF produced an IC_{50} value of 29 μM (Figure 1C).

Development of Second-Generation BRAF Inhibitors. Upon closely examining the molecular structure of compound **1**, we noted that the hexahydropteridine portion of the molecule contained two symmetrical methylpyridinium groups at opposite ends which suggests that the hexahydropteridine portion and only one of the two methylpyridinium groups might be employed in BRAF inhibition (Figure 1a). To obtain more direct insight into the binding mode of compound **1** to BRAF, we analyzed its docked conformation within the BRAF active site (Figure 1b). This docking result revealed that one of the methylpyridinium groups and the hexahydropteridine portion of the molecule interacted with the BRAF active site through extensive hydrophobic interactions with BRAF active-site residues Trp463, Val471, Leu514, Trp531, and Phe583. In contrast, the second methylpyridinium group pointed outside of the BRAF active site and had minimal interactions with the protein. On the basis of this observation, we hypothesized that the inhibitory activity of compound **1** was largely due to the hexahydropteridine moiety combined with only one of the two methylpyridinium groups of compound **1**. To test this hypothesis, we derived a new scaffold named compound **1a** (Figure 1a) that consisted of only the hexahydropteridine and methylpyridinium groups as a query to search the SPECS database for compounds with similar scaffolds. From this approach, compound **19** was identified and tested by the use of the BRAF ELISA assay for inhibitory activity against BRAF. Consistent with our hypothesis, compound **19**, which has a purine-2,6-dione scaffold that is similar to that of our query structure, was indeed a relatively potent BRAF inhibitor and showed a 90% reduction of BRAF activity at an inhibitor concentration of 50 μM. A dose−response inhibition curve of compound **19** against BRAF produced an IC_{50} value of 2.1 μM (Figure 1c and Table 1).

On the basis of the positive results that were obtained with compound **19**, we used it as a query scaffold and identified compounds **22**−**41** (Table 1 and Figure S1c in the Supporting Information) as close analogues of compound **19**. From these compounds, we identified compound **24** (Figure 2a), which showed inhibition against BRAF with an IC_{50} value of 1.7 μM (Figure 2b and Table 1). Taken together, our in vitro assay results established compound **24** as the most potent BRAF inhibitor within this library of compound **19** analogues.

Selectivity of Compound 24 for BRAF. To probe the kinase selectivity of compound **24** against BRAF over other kinases, we selected six kinases, PI3Kγ, GSK3β, Pim1, MST1, PAK1, and PAK4, which represent four major kinase families of lipid kinases and CMGC, CAMK, and STE protein kinases. As shown in Figure 2c, compound **24** did not show significant inhibition against GSK3β, Pim1, MST1, PAK1, and PAK4 at an inhibitor concentration of 100 μM, and it showed PI3Kγ inhibition with an IC_{50} value of only 25 μM. Therefore, our data establish compound **24** as a BRAF inhibitor with more than a 50-fold selectivity over other representative protein kinases and more than a 12-fold selectivity over PI3K lipid kinases. Taken together, our kinase profiling data suggested that the HTVS approach described here can lead to the identification of low micromolar BRAF inhibitors with significant kinase-inhibitor selectivity.

Molecular Modeling of BRAF Inhibitors. To understand the mode of inhibition of compounds **19** and **24** to BRAF, we docked these compounds into the active site of BRAF by using AutoDock3.0. As shown in Figure 4a, compound **19** is modeled to bind the ATP-binding pocket of BRAF such that one of the carbonyl oxygen atoms of the purine-2,6-dione ring forms a hydrogen bond with the amide nitrogen of residue Cys532 in the hinge region between the N lobe and C lobe of the BRAF kinase domain. In addition, the model suggests that extensive

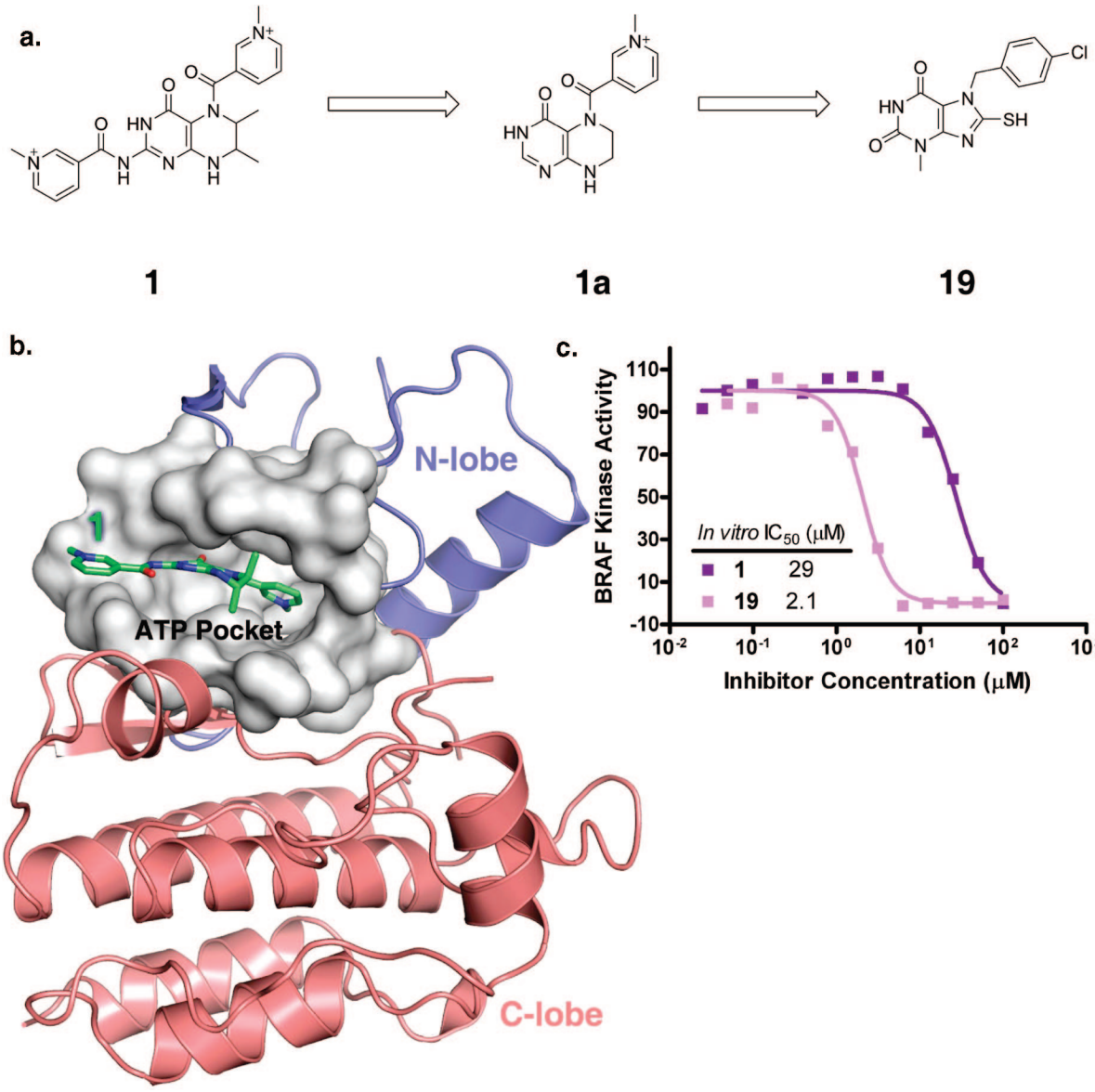

Figure 1. Identification of compounds **1** and **19** as BRAF inhibitors. (a) Molecular structures of compound **1**, symmetry-extracted scaffold **1a**, and compound **19**. (b) Binding mode of compound **1** in the active site of the BRAF protein kinase. The surface representation is white to show all ATP pocket residues within 8 Å of compound **1**. The N lobe and C lobe of the BRAF kinase domain are blue and red, respectively. (c) Dose−response curve of BRAF kinase inhibition by compounds **1** (purple) and **19** (pink) by the use of an in vitro BRAF ELISA kinase assay.

hydrophobic interactions are formed between compound **19** and the ATP-binding pocket of BRAF kinase. In particular, residues Ile463, Ser466, Val471, Ala481, Val482, Lys483, Leu514, Thr529, Trp531, Phe583, and Phe595 are predicted to make van der Waals contacts with compound **19**.

In contrast to compound **19**, compound **24** is modeled to bind to the BRAF active site in a different orientation, which is apparently due to the bulky phenyl group derivatization on the maleimide nitrogen of the purine-2,6-dione ring (Figure 3b). Nonetheless, this phenyl group is predicted to bind essentially the same hydrophobic pocket as targeted by the chlorophenyl moiety of compound **19**. In addition to extensive hydrophobic interactions that are predicted to form between BRAF and compound **24** with residues Ile463, Val471, Ala481, Ile527, Lys483, Leu514, Thr529, Trp531, Cys532 and Phe583, compound **24** also is modeled to make two additional hydrogen bonding interactions with Thr529 and Gly534 of BRAF. In particular, the thioethanol group of compound **24** forms hydrogen bonds with the amide carbonyl of Gly534 and the maleimide carbonyl of compound **24** also interacts with the side chain of Thr529 by forming a potential hydrogen bond. This model can also explain why compound **24** is a more potent inhibitor than compound **23** (Table 1).

Comparison with other BRAF Inhibitors. Several BRAF inhibitors that were identified through solution screening have been described in the literature including a bisaryl urea compound, **51**,[13] and a triarylimidazole derivative, compound **50**.[7] Although these compounds bind more potently to BRAF than do compounds **19** and **24** that are described here (Table S2 in the Supporting Information) through in silico screening, there are some interesting similarities and differences, particularly with compound **50**, that might be exploited to improve the BRAF potency of compounds **19** and **24** for BRAF. In particular, a comparison of **19** and **24** inhibitors with compound **50** in complex with BRAF[7] shows significant similarities in their BRAF binding modes (Figure 3c). Like the compound **50** inhibitor, the purine-2,6-dione ring of both compound **19** and compound **24** intercalates between residues F583 and W531 by making a $\pi-\pi$ stacking interaction.[7] In addition, the chlorophenyl moiety of compound **19** and the phenyl group of compound

Table 1. Molecular Structures of Compounds That Show Inhibitory Activity against $BRAF^{WT}$

Compound	Structure	IC_{50} for $BRAF^{WT}$ (μM)	Compound	Structure	IC_{50} for $BRAF^{WT}$ (μM)
1	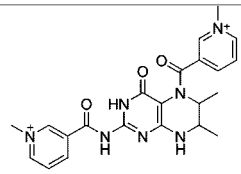	29.42	**28**	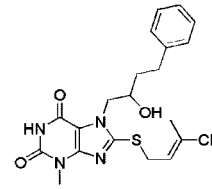	3.75
19	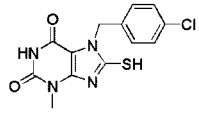	2.10	**29**	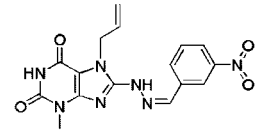	37.48
22	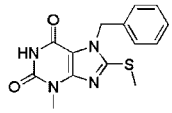	30.11	**30**	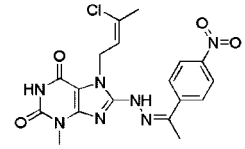	17.36
23	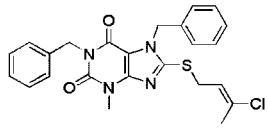	10.91	**31**	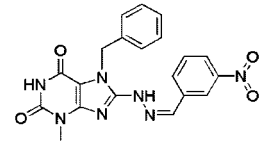	>50
24	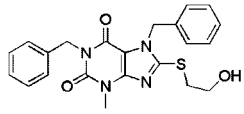	1.72	**32**	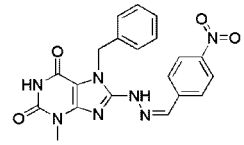	57.89
25	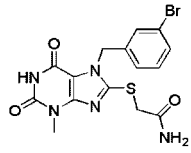	11.08	**33**	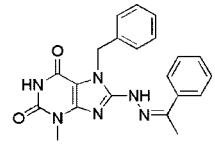	11.36
26	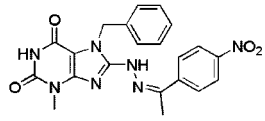	4.60			
27	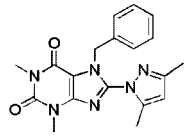	57.71			

24 adopt orientations that are similar to the indane-oxime group of compound **50** within the BRAF-binding pocket, which has the bulky group pointing toward the BRAF-activation loop where it may play an important role in BRAF selectivity.[7,14] The chlorophenyl group of compound **19** and the phenyl group of compound **24** occupy significantly less space within the BRAF active site than does the corresponding indane-oxime group of compound **50** (Figure 3c). On the basis of this observation, we propose that analogues of compounds **19** and **24** that contain additional hydrophilic modifications in this position may mediate additional protein interaction and shape complementarity near the activation loop, and this strategy would likely increase BRAF inhibitor potency and specificity (Figure 4).

Our SAR analysis also reveals that bulkier substitutions on the thiol moiety significantly reduce BRAF inhibitor potency. For example, compounds **31** and **32** which contain a nitrophenylhydrazine group in this position, show at least a 20-fold reduction in BRAF inhibitor potency relative to compound **19** (Table 1). There are also other compounds with bulky derivatives at this position that show reduced inhibitory potency against BRAF (Table 1). These results demonstrate that compounds with bulky substitutions in this position are not favorable for BRAF inhibition.

Conclusions and Future Prospects

We have identified a series of purine-2,6-dione analogues as novel inhibitors against the BRAF kinase by using the HTVS approach from a filtered small molecule SPECS compound database that contains about 90 000 compounds. Among these newly identified purine-2,6-dione-based inhibitors, compound **1** was found to inhibit the enzymatic activity of the BRAF protein kinase in an ELISA-based MEK phosphorylation assay with an IC_{50} value of 29 μM. On the basis of the molecular docking of this compound to BRAF, a fragment scaffold (scaffold **1a** in Figure 1a) was hypothesized to be the functional moiety for BRAF inhibition. This scaffold was extracted as a query for searching structural analogues of compound **1** for testing their inhibition in an in vitro solution screen. The BRAF ELISA assay results established compound **19** from this library of analogues as a potent BRAF inhibitor with an IC_{50} value of 2.1 μM against BRAF. On the basis of the structure of this new inhibitor lead of compound **19**, 12 out of 20 compound **19** analogues were identified as low micromolar inhibitors of BRAF

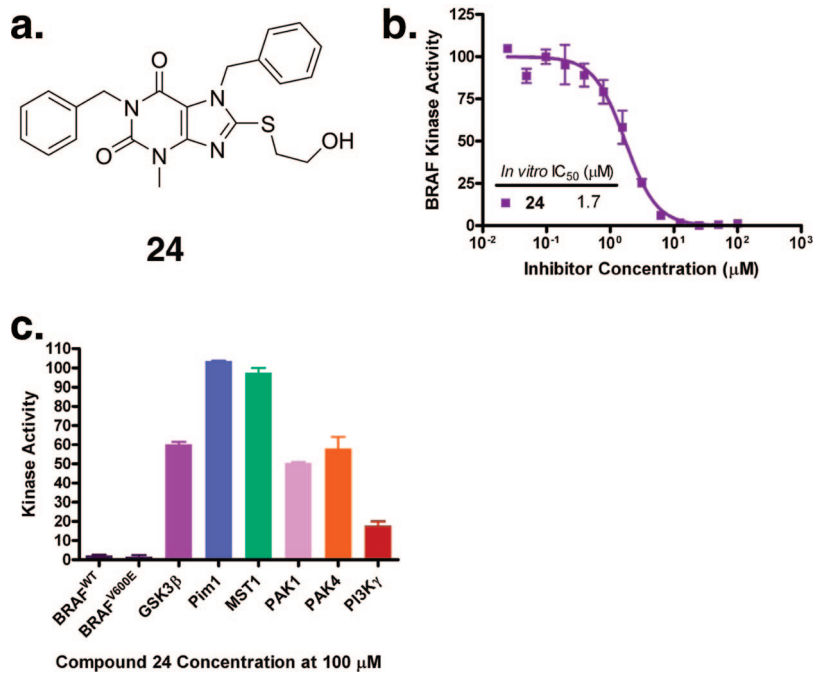

Figure 2. Identification of compound **24** as a third-generation BRAF-specific inhibitor. (a) Molecular structure of compound **24**, (b) dose−response curve of compound **24** inhibition against the BRAF kinase, and (c) kinase profiling of compound **24** against GSK3β, Pim1, PAK1, and PAK4 protein kinases and PI3Kγ lipid kinase.

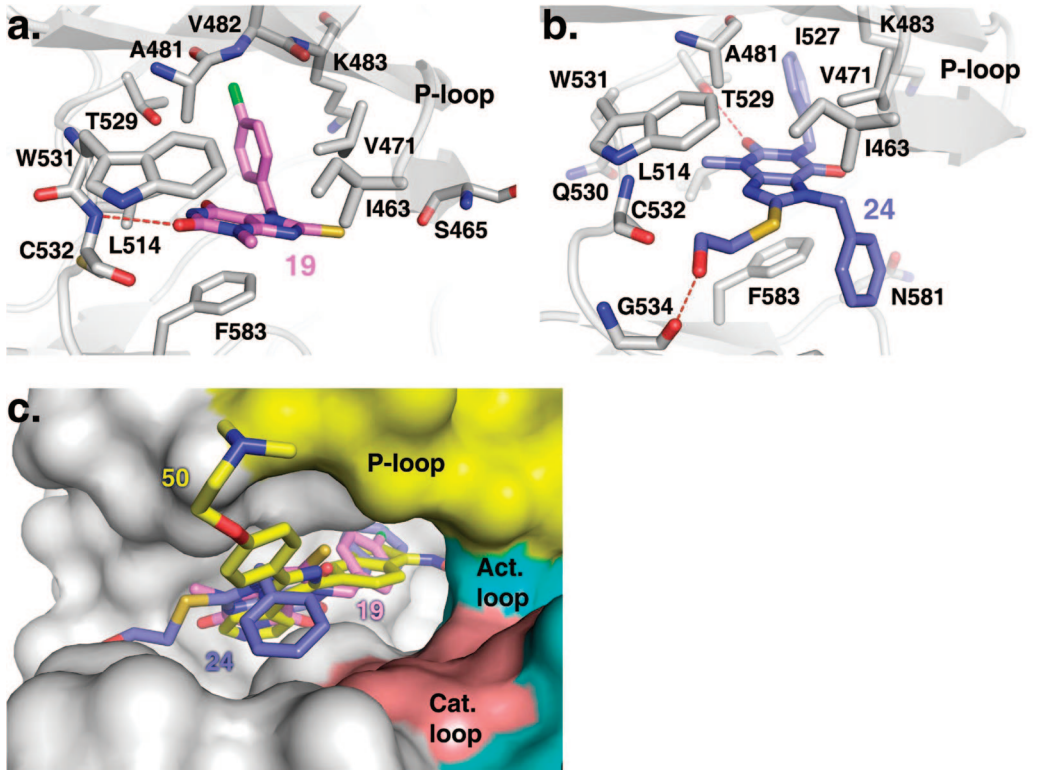

Figure 3. Docking of compounds **19**, **24**, and **50** in the BRAF active site. (a) Interactions of compound **19** with the BRAF protein kinase ATP-binding pocket. (b) Interaction of compound **24** with the BRAF protein kinase ATP-binding pocket. Hydrogen bonding interactions are represented by red dashed lines in both panel (a) and panel (b). (c) Comparison of binding modes of compounds **19** (pink), **24** (blue), and **50** (yellow) in the ATP-binding pocket of the BRAF kinase. Surface contours that correspond to the P loop, Act. (activation) loop, and Cat. (catalytical) loop are yellow, cyan, and red, respectively.

kinase. The best inhibitor, compound **24**, inhibits the kinase activity of BRAF with an IC_{50} value of 1.7 μM. We also demonstrated the selectivity of compound **24** for BRAF over other representative protein and lipid kinases in our kinase profiling studies. Furthermore, the SAR studies of inhibitor analogues and the docking studies of compounds **19** and **24** into the BRAF active site provide important pharmacophore clues for future inhibitor optimization to increase BRAF inhibitor potency and selectivity (Figure 4). In particular, compounds with modifications that extend the R_1 position of the phenyl group

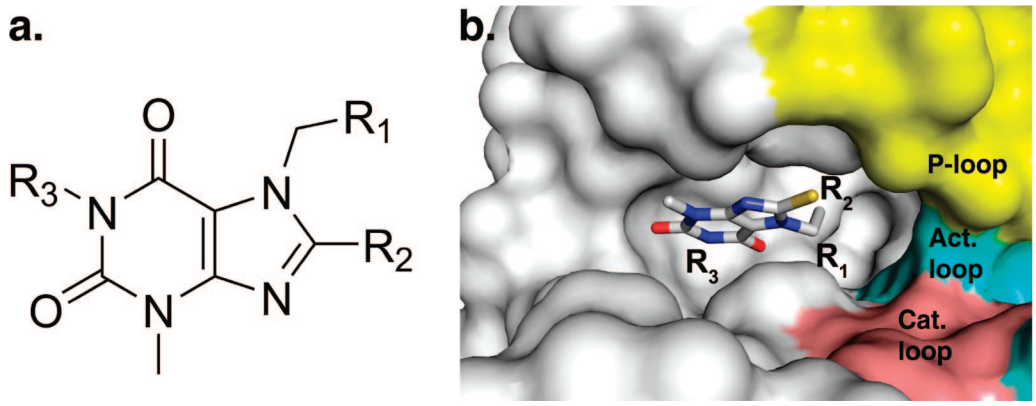

Figure 4. Future directions for designing BRAF inhibitors with greater potency and specificity. (a) Base scaffold with three possible positions for modification. (b) Corresponding position of three modification sites within the ATP-binding pocket of the BRAF protein kinase. Surface contours corresponding to the P loop, Act. loop (activation loop), and cat. loop (catalytical loop) are yellow, cyan, and red, respectively.

with a long aliphatic chain with a hydrophilic terminal end might allow the compound analogue to reach more deeply into the BRAF-binding pocket that is formed by the activation loop and the αC helix such that the hydrophilic extension interacts with residue Asp594 of BRAF (compound **28** in Table 1 and Figure S2 in the Supporting Information). The significance of this modification is underscored when one considers the fact that this pocket of the $BRAF^{V600E}$ oncogenic mutant protein may drastically differ from that of the $BRAF^{WT}$ protein because of the different conformations of the activation loop between $BRAF^{WT}$ and $BRAF^{V600E}$.[7,14] Indeed, we have shown that compounds **19** and **24** do not distinguish between $BRAF^{WT}$ and $BRAF^{V600E}$ (data not shown) which points to the potential importance of modifying the R_1 position to obtain BRAF inhibitors with isoform and oncogene specificity. The derivatization of the thiol group at the R_2 position may also increase the inhibitor-binding potency for BRAF, although large derivatizations in this position may prevent an R_1 derivatization of the phenyl group from extending into the site near the activation loop. We therefore suggest that the derivatization of the R_2 position with a relatively small substituent may be more favorable when it is combined with modifications in the R_1 position. Indeed, the SAR analysis reveals that substitutions of a bulky group in the R_2 position are not well tolerated when there is another bulky substitution in the R_1 position (compound **27** in Table 1 and compounds **34**−**36** in Figure S1c in the Supporting Information). In the R_3 position, the substitution of a bulky group, such as a phenyl, will likely change the binding conformation of the inhibitor in the BRAF ATP-binding pocket, whereas the modification of the R_3 position to a hydrophilic group will put it in the position to mediate hydrogen bonding interactions with protein pocket residues.

Our study demonstrates that an efficient and cost-effective virtual screening procedure can be used to identify potent BRAF inhibitors that also show considerable specificity for BRAF over other protein and lipid kinases. Moreover, the promising results that were obtained in this study will serve as an excellent platform for the further development of BRAF inhibitors with even greater potency and specificity for use as therapeutic agents.

Experimental Section

High-Throughput Virtual Screening. The X-ray crystal structure of the BRAF kinase domain in an active configuration[7] (PDB accession code 2FB8) was used as the target structure in this approach. The modified small molecular database that contains approximately 90 000 molecules for virtual screening was generated as a SPECS subset from the ZINC database[15] with a predicted solubility filter (log $S > -4$). The virtual screening was carried out on a four-processor Linux workstation and on the National Science Foundation Terascale Computing System at the Pittsburgh Supercomputing Center (http://www.psc.edu). A heuristic docking and consensus scoring strategy was used to evaluate the results of the virtual screening. Specifically, we used DOCK4.0 as the primary screening tool that used the active site of the BRAF/compound **50** crystal structure with the inhibitor excluded from the coordinates (PDB accession code 2FB8) as a receptor for compound binding. Residues around compound **50** at a radius of 6 Å were isolated for the construction of the grid for docking screening. This radius was large enough to include all of the residues that are involved in inhibitor binding. During the docking procedure, Kollman all-atom charges were assigned to the protein, and Geisterger−Hückel charges were assigned to the small molecules in the SPECS database. In the docking search, the conformational flexibilities of the molecules from the database were considered. We used 30 configurations per ligand-building cycle and 50 maximum anchor orientations in the anchor-first docking algorithm. All docked configurations were energy minimized by the use of 100 maximum iterations and 1 minimization cycle. Prior to screening the target molecular database, we tested this docking protocol by screening a small molecule database that contained 1000 compounds that consisted of two known BRAF inhibitors (compounds **50** and **51**) and 998 randomly selected low-molecular-weight compounds from the SPECS database, and this control experiment produced the two known BRAF inhibitors as the top-scoring ligands. Following this control experiment, we screened the target database, and the top 5000 molecules were taken as the hit list for further analysis. These molecules were reranked by the use of, in succession, XSCORE (version 1.2.1),[9] the docking and scoring mode of SLIDE (version 2.3.1),[10,11] and AutoDock3.0. On the basis of the results of these scoring functions, the molecules were ranked, and the top 200 molecules were extracted and were carefully considered for their receptor binding and scaffold diversity. We purchased 18 available candidate compounds from different scaffolds for the in vitro assay.

Molecular Docking by Autodock3.0. The molecular docking program AutoDock3.0[16] was used for the automated molecular docking simulations. The docking scheme is summarized as follows. First, the BRAF receptor molecule was checked for polar hydrogen and was assigned for partial atomic charges. The PDBQS file was created, and the atomic solvation parameters were also assigned. The torsion angles of the docked ligands that could be sampled during the molecular docking procedure were defined to permit a conformation search for ligands during the molecular docking process. Second, a 3D search grid was created by the use of the AutoGrid algorithm[17] to evaluate the binding energies between the ligands and the BRAF receptor. The receptor was embedded in the 3D grid, and a probe atom was placed at each grid point. The affinity and electrostatic potential grid was calculated for various

types of atoms in the ligands. The energetic configuration of a particular ligand was determined by the use of trilinear interpolation of affinity values and the electrostatic interaction of the eight grid points around each atom of the ligand. Third, a series of the docking parameters was defined. The atom types, the generations, and the run numbers for the LGA algorithm were properly assigned according to the requirement of the Amber force field. The generations, energy evaluations, and docking run numbers were set as 370 000, 1 500 000, and 20, respectively. Kollman all-atom charges were assigned for the BRAF receptor and Gasteiger−Marsili[18] charges were assigned for the ligands. Finally, the docked ligand−receptor complexes were selected according to the criteria of interacting energy combined with geometrical matching quality. These complexes were used as the starting conformation for further energetic minimization and geometrical optimization before the final binding models were generated.

Cloning, Protein Expression, and Purification. The full-length human BRAF clone was kindly provided by Dr. Richard Marais (Institute of Cancer Research, U.K.), and the full-length mouse p50cdc37 clone was provided by Dr. Wade Harper (Harvard Medical School). The human BRAF kinase domain (residues 433−726) with an N-terminal purification tag ($MDRGSH_6GS$) and the full-length mouse $p50^{cdc37}$ were PCR-amplified and subcloned into the pFastBac dual vector. The BRAF kinase domain was expressed and purified essentially as previously described.[3]

In Vitro BRAF Kinase Assay. Recombinantly expressed GST-MEK that was diluted in TTBS buffer (20 mM Tris pH 7.5, 150 mM NaCl, 0.05% TWEEN-20) to 50 μg/mL was bound in 100 μL volume to the wells of a 96-well glutathione-coated plate (Pierce Biotechnology). A compound with 2× serial dilutions in 100% DMSO stock (1 μL) was added to a mixture of 50 μL of 50 mM HEPES (pH 7.0) with BRAF kinase (25 ng). This mixture was incubated at room temperature for 1 h before it was added to the GST-MEK-treated wells of the 96-well plate. An additional 50 μL of phosphorylation buffer (50 mM HEPES pH 7.0, 200 mM NaCl, 10 mM $MgCl_2$, 200 μM ATP) was added to this mixture to start the kinase reaction at 37 °C for 30 min with intermittent shaking. The kinase reaction was stopped by extensive washing with TTBS buffer, and a 1:5000 dilution of antiphospho-MEK1 (Ser218/222)/MEK2 (Ser222/226) monoclonal antibody (Millipore) in TTBS was subsequently added to the wells, and the mixture was incubated for 1 h with shaking. Goat anti-rabbit IgG (H + L)-HRP conjugate (BioRad Laboratories) in a 1:5000 dilution was added to the wells, and the mixture was incubated at room temperature with shaking. The SuperSignal ELISA pico chemiluminescent substrate (Pierce Biotechnology) was added to the wells. The luminescence signal was recorded by a luminescence filter by a Wallac 1420 luminometer (PerkinElmer). These data were processed, and IC_{50} values were derived from the sigmoidal dose−response curve fitting by GraphPad Prism 4.0.

Acknowledgment. We thank Dr. M.Y. Zheng from the Shanghai Institute of Materia Medica of the Chinese Academy of Sciences for kindly providing the ZlogS program for the solubility prediction on the small molecules in the SPECS database. We also thank Dr. Ruchi Anand for carrying out the MST1 kinase assay and Jasna Maksimoska for carrying out the GSK3β, Pim1, PAK1, and PAK4 kinase assays. We thank Dr. Richard Marais for providing the full-length human BRAF clone and Dr. Wade Harper for providing the full-length mouse clone. We thank the Wistar Protein Expression facility for preparing recombinant proteins. This work was supported by NIH grant CA114046.

Supporting Information Available: ^{1}H NMR spectra for all described compounds, PI3Kγ, GSK3β, MST1, Pim1, PAK1, and PAK4 kinase assay procedures, a consensus ranking of 18 initial hits from HTVS, a comparison of compound **24** with conventional BRAF kinase inhibitors, and additional references. This material is available free of charge via the Internet at http://pubs.acs.org.

References

(1) Sridhar, S. S.; Hedley, D.; Siu, L. L. Raf kinase as a target for anticancer therapeutics. *Mol. Cancer Ther.* **2005**, *4*, 677–685.
(2) Garnett, M. J.; Marais, R. Guilty as charged: B-RAF is a human oncogene. *Cancer Cell* **2004**, *6*, 313–319.
(3) Wan, P. T.; Garnett, M. J.; Roe, S. M.; Lee, S.; Niculescu-Duvaz, D.; Good, V. M.; Jones, C. M.; Marshall, C. J.; Springer, C. J.; Barford, D.; Marais, R. Mechanism of activation of the RAF-ERK signaling pathway by oncogenic mutations of B-RAF. *Cell* **2004**, *116*, 855–867.
(4) Ahmad, T.; Eisen, T. Kinase inhibition with BAY 43−9006 in renal cell carcinoma. *Clin. Cancer Res.* **2004**, *10*, 6388S–6392S.
(5) Vangrevelinghe, E.; Zimmermann, K.; Schoepfer, J.; Portmann, R.; Fabbro, D.; Furet, P. Discovery of a potent and selective protein kinase CK2 inhibitor by high-throughput docking. *J. Med. Chem.* **2003**, *46*, 2656–2662.
(6) Siddiquee, K.; Zhang, S.; Guida, W. C.; Blaskovich, M. A.; Greedy, B.; Lawrence, H. R.; Yip, M. L. R.; Jove, R.; McLaughlin, M. M.; Lawrence, N. J.; Sebti, S. M.; Turkson, J. Selective chemical probe inhibitor of Stat3, identified through structure-based virtual screening, induces antitumor activity. *Proc. Natl. Acad. Sci. U.S.A.* **2007**, *104*, 7391–7396.
(7) King, A. J.; Patrick, D. R.; Batorsky, R. S.; Ho, M. L.; Do, H. T.; Zhang, S. Y.; Kumar, R.; Rusnak, D. W.; Takle, A. K.; Wilson, D. M.; Hugger, E.; Wang, L.; Karreth, F.; Lougheed, J. C.; Lee, J.; Chau, D.; Stout, T. J.; May, E. W.; Rominger, C. M.; Schaber, M. D.; Luo, L.; Lakdawala, A. S.; Adams, J. L.; Contractor, R. G.; Smalley, K. S.; Herlyn, M.; Morrissey, M. M.; Tuveson, D. A.; Huang, P. S. Demonstration of a genetic therapeutic index for tumors expressing oncogenic BRAF by the kinase inhibitor SB-590885. *Cancer Res.* **2006**, *66*, 11100–11105.
(8) Kuntz, I. D.; Meng, E. C.; Shoichet, B. K. Structure-based molecular design. *Acc. Chem. Res.* **1994**, *27*, 117–123.
(9) Wang, R.; Lu, Y.; Wang, S. Comparative evaluation of 11 scoring functions for molecular docking. *J. Med. Chem.* **2003**, *46*, 2287–2303.
(10) Zavodszky, M. I.; Sanschagrin, P. C.; Korde, R. S.; Kuhn, L. A. Distilling the essential features of a protein surface for improving protein-ligand docking, scoring, and virtual screening. *J. Comput. Aided Mol. Des.* **2002**, *16*, 883–902.
(11) Schnecke, V.; Swanson, C. A.; Getzoff, E. D.; Tainer, J. A.; Kuhn, L. A. Screening a peptidyl database for potential ligands to proteins with side-chain flexibility. *Proteins* **1998**, *33*, 74–87.
(12) Goodsell, D. S.; Morris, G. M.; Olson, A. J. Automated docking of flexible ligands: applications of AutoDock. *J. Mol. Recognit.* **1996**, 1–5.
(13) Wilhelm, S. M.; Carter, C.; Tang, L.; Wilkie, D.; McNabola, A.; Rong, H.; Chen, C.; Zhang, X.; Vincent, P.; McHugh, M.; Cao, Y.; Shujath, J.; Gawlak, S.; Eveleigh, D.; Rowley, B.; Liu, L.; Adnane, L.; Lynch, M.; Auclair, D.; Taylor, I.; Gedrich, R.; Voznesensky, A.; Riedl, B.; Post, L. E.; Bollag, G.; Trail, P. A. BAY 43−9006 exhibits broad spectrum oral antitumor activity and targets the RAF/MEK/ERK pathway and receptor tyrosine kinases involved in tumor progression and angiogenesis. *Cancer Res.* **2004**, *64*, 7099–7109.
(14) Tsai, J.; Lee, J. T.; Wang, W.; Zhang, J.; Cho, H.; Mamo, S.; Bremer, R.; Gillette, S.; Kong, J.; Haass, N. K.; Sproesser, K.; Li, L.; Smalley, K. S.; Fong, D.; Zhu, Y. L.; Marimuthu, A.; Nguyen, H.; Lam, B.; Liu, J.; Cheung, I.; Rice, J.; Suzuki, Y.; Luu, C.; Settachatgul, C.; Shellooe, R.; Cantwell, J.; Kim, S. H.; Schlessinger, J.; Zhang, K. Y.; West, B. L.; Powell, B.; Habets, G.; Zhang, C.; Ibrahim, P. N.; Hirth, P.; Artis, D. R.; Herlyn, M.; Bollag, G. Discovery of a selective inhibitor of oncogenic B-Raf kinase with potent antimelanoma activity. *Proc. Natl. Acad. Sci. U.S.A.* **2008**, *105*, 3041–3046.
(15) Irwin, J. J.; Shoichet, B. K. ZINC: a free database of commercially available compounds for virtual screening. *J. Chem. Inf. Model.* **2005**, *45*, 177–182.
(16) Morris, G. M.; Goodsell, D. S.; Huey, R.; Hart, W. E.; Halliday, R. S.; Belew, R. K.; Olson, A. J., *AutoDock*, version 3.0.3; The Scripps Research Institute, Molecular Graphics Laboratory, Department of Molecular Biology: La Jolla, CA, 1999.
(17) Morris, G. M.; Goodsell, D. S.; Halliday, R. S.; Huey, R.; Hart, W. E.; Belew, R. K.; Olson, A. J. Automated docking using a Lamarckian genetic algorithm and and empirical binding free energy function. *J. Comput. Chem.* **1999**, *19*, 1639–1662.
(18) Gasteiger, J.; Marsili, M. Iterative partial equalization of orbital electronegativity: a rapid access to atomic charges. *Tetrahedron* **1980**, *36*, 3219–3228.

JM800539G